Available online at www.sciencedirect.com
ScienceDirect
Journal of Power Sources 172 (2007) 67–71
JOURNAL OF POWER SOURCES
www.elsevier.com/locate/jpowsour

Short communication

Feasibility of liquid hydrocarbon fuels for SOFC with Ni–ScSZ anode

Haruo Kishimoto*, Katsuhiko Yamaji, Teruhisa Horita, Yueping Xiong, Natsuko Sakai, Manuel E. Brito, Harumi Yokokawa

National Institute of Advanced Industrial Science and Technology (AIST), AIST Tsukuba Central No. 5, Higashi 1-1-1, Tsukuba, Ibaraki 305-8565, Japan

Received 30 October 2006; received in revised form 22 March 2007; accepted 17 April 2007
Available online 25 April 2007

Abstract

Solid oxide fuel cell (SOFC) operation with a nickel–scandia stabilized zirconia (Ni–ScSZ) cermet anode was carried out with liquid hydrocarbon of *n*-dodecane ($C_{12}H_{26}$), used as a model fuel of kerosene, without fuel dilution by inert carrier gas. Continuous operation was achieved for more than 120 h at S/C = 2.0 and at 800 °C. The obtained open circuit voltage was about −0.97 V and the average current density was about 140 mA cm^{-2} under the constant anode potential of −0.75 V versus air. This current density corresponded to fuel utilization of 55%. In the impedance spectra for the anode, two semicircles were observed not only for hydrogen but also for C1 to C12 paraffin. Electrode conductivity for each semicircle, σ_H for high frequency part and σ_L for low frequency part, were calculated by following equation:

$$\sigma\,(\mathrm{S\,cm^{-2}}) = \frac{1}{AR}$$

where A (cm^2) is electrode area and R (Ω) is electrode resistance determined from each semicircle. Electrode conductivities for hydrocarbon fuels showed the same water partial pressure dependence as that for hydrogen whether fuel is diluted or not. Hydrogen produced by reforming reaction was the most active element for electrochemical oxidation at the anode even for hydrocarbon fuels.

Keywords: Solid oxide fuel cell (SOFC); Liquid hydrocarbon; Anode; Nickel; Scandia stabilized zirconia (ScSZ); Reaction process

1. Introduction

Solid oxide fuel cells (SOFCs) are strong candidates to become the most efficient electricity generation system. In SOFC, oxygen is reduced at cathode, oxide ion is transported through the electrolyte and fuel is oxidized at the anode at high temperature, ranging between 600 and 1000 °C. This basic principle of SOFCs operation implies that not only hydrogen but also many kinds of fuels, such as hydrocarbons, can be directly used as fuel. There are several ways to use hydrocarbon fuels for SOFCs. One is by external reforming, the second is by internal reforming and the other, and very important one, is fuel reforming directly on the anode. By the last method, the heat generated by electrochemical oxidation reaction can be used most effectively for the reforming reaction. At the same time, it does not require any precious metal for reforming catalyst, and the overall stack and system will be simplified. From these features, the highest efficiency can be expected for SOFCs designed to reform fuels directly on the anode. As a drawback, carbon deposition on the anodes and in the feeding tubes becomes a serious problem. It is important to recognize that when conventional nickel–yttria stabilized zirconia (Ni–YSZ) cermet anode is used for hydrocarbon fuel feeding without previous reforming, carbon deposition occurs and leads to anode degradation [1,2].

In Japan, kerosene is consumed in very large amount for house using, especially for heating and hot water supply [3]. The kerosene-supplying infrastructure has been already well developed. Needless to say that liquid hydrocarbons are easy to distribute and to storage and have a high energy density per volume, and that their use is widespread in rural areas. On the other hand, the gas fuel distribution network covers only city areas. Therefore, it is natural to think that kerosene will be come an important fuel for practical use of SOFCs in Japan. To make it possible the use of liquid hydrocarbons in SOFCs,

* Corresponding author. Tel.: +81 29 861 4542; fax: +81 29 861 4540.
E-mail address: haruo-kishimoto@aist.go.jp (H. Kishimoto).

0378-7753/$ – see front matter © 2007 Elsevier B.V. All rights reserved.
doi:10.1016/j.jpowsour.2007.04.042

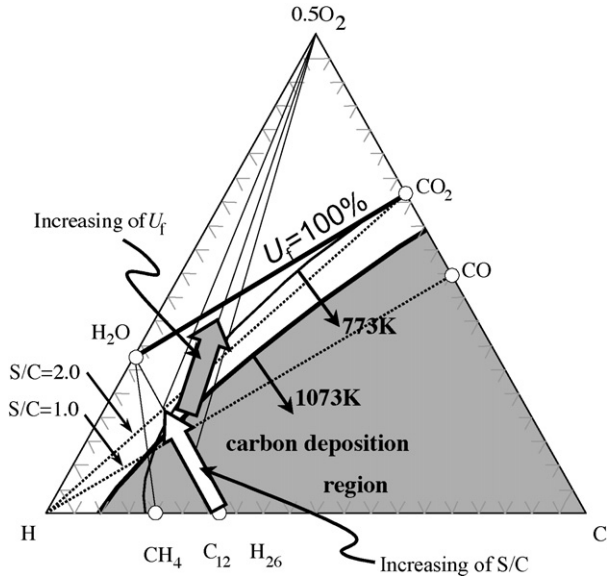

Fig. 1. Equilibrium phase diagram for the C–H–O ternary system. A hatched area shows the carbon deposition region at 800 °C.

it is important to avoid carbon deposition on the anode and to promote reforming reactions. Important information to avoid carbon deposition was suggested from thermodynamic calculation. Fig. 1 shows the equilibrium phase diagram for the C–H–O ternary system. The hatched area shows the carbon deposition region at 800 °C. It is clear that carbon deposition become critical for higher hydrocarbons. On the other hand, at a high steam to carbon ratio (S/C) region, or at a high fuel utilization (U_f) region, the carbon deposition is avoidable.

The SOFC operating with direct feeding of hydrocarbon fuels without reformer have been reported for methane with a nickel–scandia stabilized zirconia (Ni–ScSZ) cermet anode [4,5] and for liquid hydrocarbons with a Cu–CeO_2–YSZ anode [2,6,7]. We have succeeded in a stable operation of SOFC with the Ni–ScSZ anode for more than 150 h, using a *n*-dodecane ($C_{12}H_{26}$, model fuel of kerosene) with dilution by inert gas [8–10]. Neither carbon deposition on the Ni–ScSZ anode nor on the gold or nickel mesh current collector was observed. However, under the fuel-diluted condition, carbon deposition could be suppressed owing to the low fuel concentration which is a condition far from practical usage. In the present study, we intended to operate a SOFC with the Ni–ScSZ anode under more practical condition, i.e. without inert gas as a diluent. For this purpose we have used *n*-dodecane ($C_{12}H_{26}$) as a model fuel of kerosene. Similarities in the reaction process between hydrogen and hydrocarbon fuels and the influence of fuel dilution on the reaction process were also examined.

2. Experimental

The half-cell used in the present study is the same as the previous reports [8–10]. Electrolyte disks (0.5 mm thickness) were prepared from commercial powder of 10 mol% Sc_2O_3–1 mol% CeO_2–89 mol% ZrO_2 (ScSZ, Daiichi Kigenso Kagaku Kogyo Co. Ltd.). 50 vol.% Ni–ScSZ cermet anode was used. NiO–ScSZ mixed powder calcined at 1573 K was painted on the polished electrolyte surface with 10 mm diameter and fired at 1673 K for 5 h. Platinum (Pt) paste was fired on the opposite side of the electrolyte as cathode and Pt wire was attached on the side edge of the electrolyte as reference electrode (RE). Dry air fed to the cathode and RE was exposed to the air.

For introduction of *n*-dodecane without diluent, *n*-dodecane and water were fed to the anode by using syringe pump with a small constant flow rate of 0.382 μl min^{-1} (1.68 μmol min^{-1}) and 0.734 μl min^{-1} (40.8 μmol min^{-1}), respectively, to realize the high U_f. The fuel was changed from the H_2–H_2O–Ar mixture to *n*-dodecane (S/C = 2.0) by the following step: (1) H_2–H_2O–Ar mixture was fed to the anode. At this time, water was supplied by syringe pump. (2) *n*-Dodecane was pumped into the anode chamber. (3) H_2 was stopped. (4) Carrier gas (Ar) was stopped under the cell operation. The cell configuration for the test without dilution is shown in Fig. 2.

To investigate the effect of carbon number on the reaction process, methane (CH_4), propane (C_3H_8), *n*-octane (C_8H_{18}) and *n*-dodecane ($C_{12}H_{26}$) are used as model fuels of city gas, LPG, gasoline and kerosene, respectively. Fuel concentrations for diluted feeding of various hydrocarbons are listed in Table 1. Fuels were diluted with argon gas to about 2 vol.%. Detail of feeding method of diluted liquid hydrocarbons was described in earlier reports [8–10].

Electrochemical measurements for anode versus RE of impedance measurement and anodic polarization measurement were carried out with an electrochemical interface and an impedance/gain-phase analyzer (Solartron, 1287A and 1255B, Hampshire, UK) or electrochemical measurement system (Hokuto Denko, HZ-3000, Tokyo, Japan). Impedance spectra were measured in the frequency range from 50,000 to

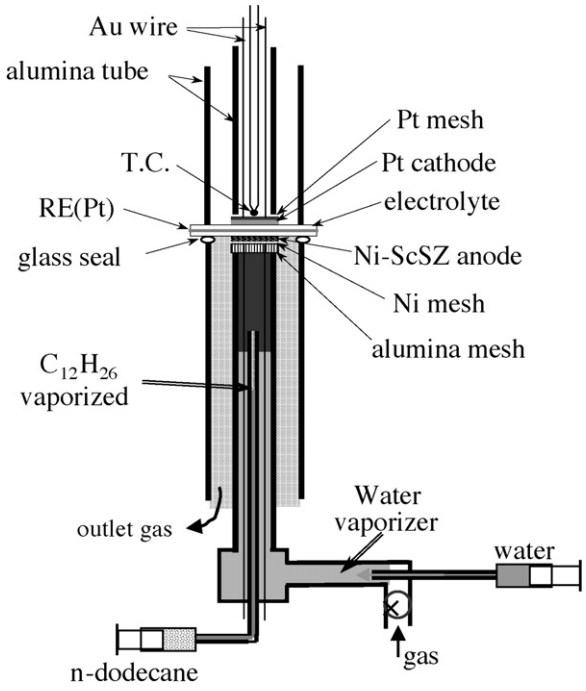

Fig. 2. Schematic drawing of the cell configuration for the cell test without inert gas fuel diluent.

Table 1
Flow rates of hydrocarbon fuels and water, and S/C ratio for each hydrocarbon fuel

Fed fuel	Fuel (μmol min^{-1})	Water (μmol min^{-1})	S/C
Methane, CH_4	15.5	31.1	2.0
Propane, C_3H_8	5.4	35.9	2.3
n-octane, C_8H_{18}	2.4	39.0	2.0
n-dodecane, $C_{12}H_{26}$	1.9	43.7	1.9

Fuels were diluted by 50 ml min^{-1} of argon gas.

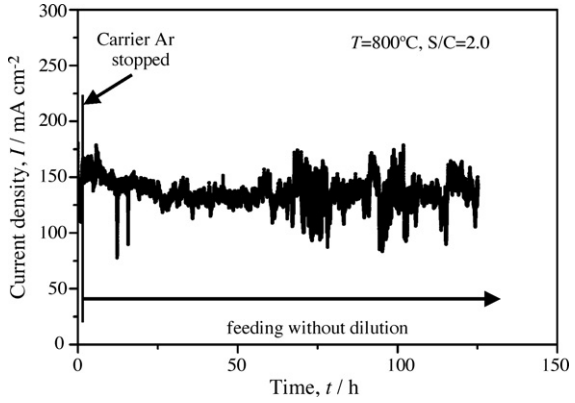

Fig. 3. The result of current density measurement with *n*-dodecane fuel without inert gas diluent at S/C = 2.0 and at T = 800 °C. Anode potential was set at constant value of −0.75 V vs. RE (air).

0.1 Hz. The outlet gas was analyzed with a gas chromatography (Agilent Technologies, Micro GC 3000, CA, USA), a dew point meter (Vaisala, DM-500, Helsinki, Finland, or General Eastern Instruments, Optica, MA, USA) and a film flow meter (STEC, SF-1, Kyoto, Japan).

3. Results and discussion

3.1. Cell operation with n-dodecane without inert gas diluent

Fig. 3 shows the result of current density measurement for direct feeding of *n*-dodecane without inert gas diluent at S/C = 2 under the potentiostatic condition with constant anode potential of −0.75 V versus RE (air) at 800 °C. The open circuit voltage (OCV) in this measurement was about −0.97 V and this value was about the same as previous diluted feeding test [9,10]. After carrier gas was stopped at t = 1 h, continuous operation was achieved for more than 120 h. The average current density was about 140 mA cm^{-2}, which corresponded to 55% of fuel utilization (U_f). The output power for the cell test without dilution was also about the same as that for previous diluted test [9,10]. In this measurement, the current density fluctuation became large for about 10 h around t = 75, 100 and 120 h. The fluctuations were synchronized with the air conditioner (AC) cycle in the laboratory. Hence, the surrounding conditions of the experimental equipment, such as temperature and atmospheric pressure, are affected; especially flow rates of fuel and water, which were very small, are sensitive to the experimental environment. After this measurement, carbon deposition was observed only on the inside of the inlet tube, however, no carbon deposition was observed on the Ni–ScSZ anode nor the nickel mesh current collector. It is clear that the Ni–ScSZ anode can survive without carbon deposition on the anode under the direct feeding of liquid hydrocarbon fuel without inert gas as diluent when the S/C is enough high as 2.0 and the U_f is as high as 50%.

Table 2 shows the result of the outlet gas analysis under the operation without dilution at the U_f = 46% compared with that of the diluted test at similar U_f of 44% [9,10]. The present result shows that the hydrogen concentration and CO_2/CO ratio were higher and C2 hydrocarbon concentration was lower than the result for diluted test. This suggests that CO shift reaction and hydrocarbon reforming reaction, except methane, were promoted for direct feeding of *n*-dodecane without inert gas diluent. This behavior should be related to the increase of contact time between fuel molecules and nickel surface because of lower flow rate (about 1/25) compared with the diluted test, and/or higher P_{H_2O} around the nickel surface as shown in Table 2.

3.2. Anode reaction process

Fig. 4(a) and (b) shows the impedance spectra for the anode with various fuels of diluted methane, propane, *n*-octane and *n*-dodecane (a), and of hydrogen and *n*-dodecane with and without diluent (b). All results were obtained about the anode against RE (air), so the resistance for cathode were not included. Ohmic resistances (R_Ω) were almost the same for all fuels. In all impedance spectra, there were two semicircles for electrode resistance; the left side electrode resistance was at high frequency (indicated as R_H), and that at right side was at low frequency (indicated as R_L). The top of each semicircle was at about 1 kHz for R_H and about 1 Hz for R_L, respectively, for the Ni–ScSZ anode and these values were about the same among hydrogen and hydrocarbon fuels. From Fig. 4(a), the features of spectra were the same for all hydrocarbon fuels with about the same fuel concentration as listed in Table 1. This suggests that the rate determining process related to each

Table 2
Outlet gas concentration under the U_f = 46% operation for the *n*-dodecane fueled cell test at S/C = 2.0 without inert gas diluent compared with that for diluted test under the U_f = 45% operation

	H_2 (%)	H_2O (%)	CO (%)	CO_2 (%)	CH_4 (%)	C_2H_4 (%)	C_2H_6 (%)
Without diluent (U_f = 46%)	29.5	46.5 (P_{H_2O} = 47 kPa)	5.2	16.3 (CO_2/CO = 3.1)	2.4	0.1	0
Diluted fuel (U_f = 45%)	21.2	53.3 (P_{H_2O} = 2 kPa)	10.9	12.0 (CO_2/CO = 1.1)	1.9	0.9	0.1

For diluted test, inert gas (Ar) was excluded for calculation. For the test without diluent, water vapor composition was calculated from the inlet fuel composition and outlet fuel concentration.

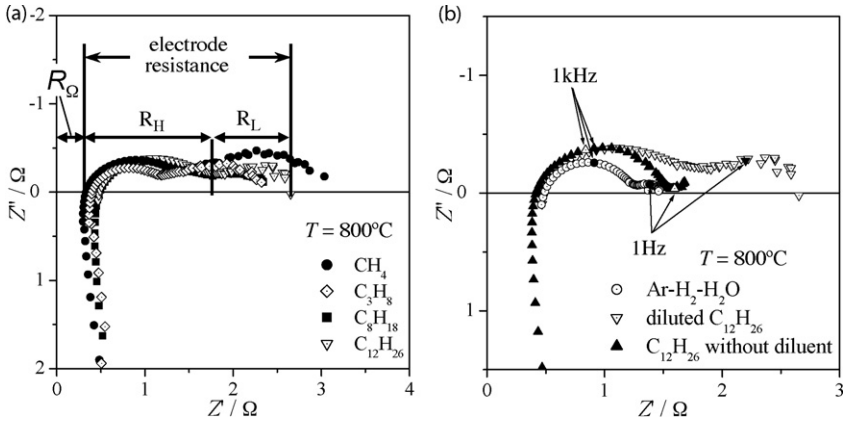

Fig. 4. Impedance spectra under the OCV condition at 800 °C for (a) diluted hydrocarbon fuels shown in Table 1 and for (b) hydrogen and *n*-dodecane with and without inert gas diluent. Impedance spectra for anode vs. RE (air) were measured. The fuel composition of hydrogen was 48.5% Ar–48.5% H_2–3% H_2O.

electrode resistance is the same, although carbon number in hydrocarbon fuels is different. On the other hand, both R_H and R_L were different among that for hydrogen and for *n*-dodecane with and without dilution as shown in Fig. 4(b). The area specific electrode conductivity, σ (S cm^{-2}), for each resistance component was calculated as following:

$$\sigma_H = \frac{1}{AR_H} \quad (1)$$

$$\sigma_L = \frac{1}{AR_L} \quad (2)$$

The apparent electrode area, A, was 0.785 cm^2. Fig. 5 shows the P_{H_2O} dependence of the σ_H and the σ_L under the OCV condition. Dashed line and dot line show the P_{H_2O} dependence of the σ_H and the σ_L, respectively, for the use of hydrogen obtained in the previous report [11]. Where the logarithmic σ_H and σ_L for hydrogen fuel were linearly increased with increasing logarithmic P_{H_2O}. The similar relation was found in σ_L between for diluted hydrocarbon fuels and for hydrogen as shown by the same closed and half closed symbols, respectively, in Fig. 5. For σ_H, slopes between diluted hydrocarbon fuels and hydrogen for the same batch anode, shown by the same open and crossed open symbols, were almost the same as that observed in hydrogen shown by dashed line. It suggested that the rate determining processes related to each electrode conductivity for diluted hydrocarbons could be regarded as the same as those for hydrogen. The electrode conductivities for *n*-dodecane without diluent were obtained from estimated P_{H_2O} and are also plotted in Fig. 5. The σ_L surely fulfilled the same relation as others. The σ_H showed slightly small value from the obtained relation for others, but the basic of the relation should be the same. These results indicate that reaction processes related to σ_H and σ_L should be essentially the same between hydrogen and hydrocarbons, whether hydrocarbons is diluted or not, and also suggest that hydrogen is the most active element for electrochemical oxidation process even for direct feeding of hydrocarbons without inert gas diluent.

It is interesting that the anode reaction process for liquid hydrocarbon fuels would be the same as that for hydrogen even under the practical condition, i.e. without inert gas diluent; hydrogen is the most active species for electrochemical oxidation reaction at the gas–nickel-electrolyte three-phase boundary (TPB). Therefore, the problems for direct feeding of hydrocarbons to the Ni–ScSZ anode can separate into some independent components although carbon number in the fuel is different and diluent is used or not. The reaction process for direct feeding of hydrocarbon fuels with water vapor to the Ni–ScSZ anode

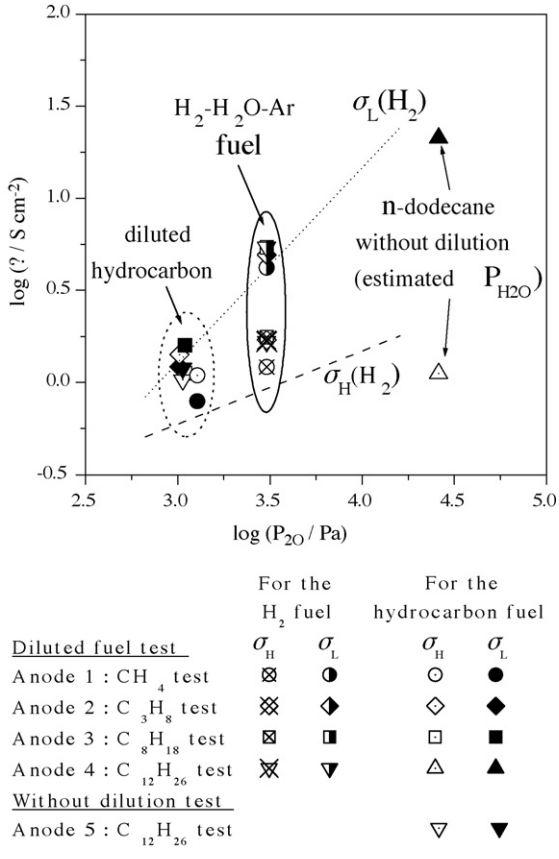

Fig. 5. Water partial pressure (P_{H_2O}) dependence of electrode conductivities of σ_H and σ_L of the Ni–ScSZ anode for hydrocarbon fuels at 800 °C. $\sigma_H = 1/AR_H$ and $\sigma_L = 1/AR_L$, respectively, where A was anode area (0.785 cm^2). For the result without diluent, P_{H_2O} was estimated from the inlet fuel composition and outlet fuel concentration. Results were compared with those with H_2–H_2O–Ar mixture fuel at 1073 K. Dot line and dashed line were the P_{H_2O} dependence of σ_H and σ_L obtained for H_2–H_2O system, respectively [11].

is summarized as follows from the previous studies [9–11]: (1) At first, hydrocarbon fuel thermally decomposes into active hydrocarbon components such as CH_3 and CH_2 at high temperature zone of the anode chamber with slight carbon deposition. (2) Active hydrocarbon components react with adsorbed water (H_2O_{ad}) and/or adsorbed oxygen (O_{ad}) on the nickel surface and as a result hydrogen and CO are formed (reforming reaction). This reaction does not proceed without nickel catalyst. The so formed CO also reacts with H_2O_{ad} and/or O_{ad} into hydrogen and CO_2 (CO shift reaction). (3) Formed hydrogen is used for electrochemical reaction at the TPB. The problems are separated as following; carbon deposition caused by thermal decomposition of hydrocarbon fuel (for the first process), acceleration of hydrogen producing reactions and its related carbon deposition (for the second process), and reduce the anode reaction resistances for electrochemical oxidation of hydrogen (at the last process).

In the present study, it becomes more serious condition for the anode after inert gas diluent was stopped during the cell operation. However, a continuous operation was achieved where carbon deposition on the anode was suppressed and hydrogen-producing reactions were promoted. We have also reported that hydrogen producing reactions are enhanced by increasing U_f rather than increasing S/C; water vapor produced by electrochemical reaction should be more effectively supplied to the nickel surface rather than that fed with fuel [11]. High U_f leads to form much water by electrochemical reaction at the TPB, and adsorption of water molecule on the nickel surface increases with increasing U_f. As a result, hydrogen-producing reactions on the Ni surface with H_2O_{ad} and/or O_{ad} are promoted and nickel surface is protected from the carbon deposition. Moreover, increasing of P_{H_2O} around the anode reduces the anodic resistances related to the anode reactions (R_L and R_H) as shown in Fig. 5. When a high U_f is realized as well as a high S/C condition, the Ni–ScSZ anode should be able to use for direct feeding of higher hydrocarbons under the practical condition, such as direct feeding of liquid hydrocarbon fuel without inert gas diluent.

4. Conclusion

Feasibility of liquid hydrocarbon fuels for SOFC with Ni–ScSZ was investigated.

Continuous operation of SOFC with the Ni–ScSZ anode is obtained for direct feeding of *n*-dodecane with water vapor without inert gas diluent under the potentiostatic condition at S/C = 2.0 at 800 °C. The averaged current density was about 140 mA cm^{-2} under the constant anode potential of −0.75 V versus RE (air) and this corresponded to 55% fuel utilization. The output power was about the same as that of previous diluted test. Rate determining processes for anode reaction was the same among hydrogen and hydrocarbon fuels; i.e. hydrogen is the most active species for electrochemical oxidation for hydrocarbon fuels whether fuel is diluted or not.

The Ni–ScSZ anode can be used for direct liquid hydrocarbon fueled SOFCs without carbon deposition on the anode with high S/C and high U_f. High U_f leads to protect the nickel from the carbon deposition because much water produced by electrochemical reaction adsorbed on the nickel surface even hydrocarbon fuel is not diluted. However, carbon deposition on the inlet tube is still a problem to be solved.

References

[1] T. Takeguchi, Y. Kani, T. Yano, R. Kikuchi, K. Eguchi, K. Tsujimoto, Y. Uchida, A. Ueno, K. Omoshiki, M. Aizawa, J. Power Sources 112 (2002) 588.
[2] R.J. Gorte, H. Kim, J.M. Vohs, J. Power Sources 106 (2002) 10.
[3] EDMC Handbook of Energy & Economic database in Japan.
[4] K. Ukai, Y. Mizutani, Y. Kume, in: H. Yokokawa, S.C. Singhal (Eds.), Proc. Solid Oxide Fuel Cells VII. The Electrochemical Society Proceedings Series, The Electrochemical Society, Pennington, NJ, 2001, p. 375, PV 2001-16.
[5] H. Sumi, K. Ukai, Y. Mizutani, H. Mori, C.-J. Wen, H. Takahashi, O. Yamamoto, Solid State Ionics 174 (2004) 151.
[6] S. Park, J.M. Vohs, R.J. Gorte, Nature 404 (2000) 265.
[7] H. Kim, S. Park, J.M. Vohs, R.J. Gorte, J. Electrochem. Soc. 148 (2001) A693.
[8] H. Kishimoto, T. Horita, K. Yamaji, Y.P. Xiong, N. Sakai, H. Yokokawa, Solid State Ionics 175 (2004) 107.
[9] H. Kishimoto, T. Horita, K. Yamaji, Y.P. Xiong, N. Sakai, H. Yokokawa, in: M. Mogensen (Ed.), Proceedings of the 6th European Solid Oxide Fuel Cell Forum, vol. 3, European Fuel Cell Forum, Oberrohrdorf, 2004, p. 1560.
[10] H. Kishimoto, T. Horita, K. Yamaji, Y.P. Xiong, N. Sakai, H. Yokokawa, J. Electrochem. Soc. 152 (2005) A532.
[11] H. Kishimoto, K. Yamaji, T. Horita, Y.P. Xiong, N. Sakai, M.E. Brito, H. Yokokawa, J. Electrochem. Soc. 153 (2006) A982.